



# CHORUS

This is the accepted manuscript made available via CHORUS. The article has been published as:

## Attractive and repulsive polymer-mediated forces between scale-free surfaces

Yacov Kantor and Mehran Kardar

Phys. Rev. E **96**, 022148 — Published 24 August 2017

DOI: [10.1103/PhysRevE.96.022148](https://doi.org/10.1103/PhysRevE.96.022148)

# Attractive and repulsive polymer-mediated forces between scale-free surfaces

Yacov Kantor<sup>1,\*</sup> and Mehran Kardar<sup>2</sup>

<sup>1</sup>*Raymond and Beverly Sackler School of Physics and Astronomy, Tel Aviv University, Tel Aviv 69978, Israel*

<sup>2</sup>*Massachusetts Institute of Technology, Department of Physics, Cambridge, Massachusetts 02139, USA*

(Dated: August 8, 2017)

We consider forces acting on objects immersed in, or attached to, long fluctuating polymers. The confinement of the polymer by the obstacles results in polymer-mediated forces that can be repulsive (due to loss of entropy) or attractive (if some or all surfaces are covered by adsorbing layers). The strength and sign of the force in general depends on the detailed shape and adsorption properties of the obstacles, but assumes simple universal forms if characteristic length scales associated with the objects are large. This occurs for scale-free shapes (such as a flat plate, straight wire, or cone), when the polymer is repelled by the obstacles, or is marginally attracted to it (close to the depinning transition where the absorption length is infinite). In such cases, the separation  $h$  between obstacles is the only relevant macroscopic length scale, and the polymer mediated force equals  $\mathcal{A}k_B T/h$ , where  $T$  is temperature. The amplitude  $\mathcal{A}$  is akin to a critical exponent, depending only on geometry and universality of the polymer system. The value of  $\mathcal{A}$ , which we compute for simple geometries and ideal polymers, can be positive or negative. Remarkably, we find  $\mathcal{A} = 0$  for ideal polymers at the adsorption transition point, irrespective of shapes of the obstacles, i.e. at this special point there is no polymer-mediated force between obstacles (scale-free or not).

PACS numbers: 64.60.F- 82.35.Lr 05.40.Fb

## I. INTRODUCTION

A prototype of soft matter, polymers are long flexible chains that can fluctuate (whether within a cell or in a solution) between a large number of configurations. The presence of hard boundaries or obstacles modifies the number and weight of allowed configurations, in turn resulting in *polymer mediated forces* between the obstacles. A well known example is the *depletion force* of polyethylene glycol (PEG) which acts to bundle filaments [1]. However, whereas the relevant length scale for depletion force is the overall size of the polymer  $R$ , here we focus on polymer-mediated forces on separations  $h \ll R$ . The internal structure of a polymer is a self-similar fractal, spanning a wide range of scales from  $R$  to a microscopic monomer size  $a$ . To compute forces between obstacles embedded in or attached to the polymer, we need to compute modifications to the free energy due to the objects. This is in principle a complex task involving the shapes of the objects, and details of their interactions with the polymer. We demonstrate that this task is considerably eased in certain cases, yielding simple universal expressions for the force.

Technological progress in manipulation of single molecules [2–6], using probes such as atomic force microscopes (AFMs) [7], microneedles [8], optical [9, 10] and magnetic [11] tweezers, makes it possible to measure forces exerted by polymers with high precision. The central motivation of these experiments is to unravel specific information about shapes, bindings, and interactions of biological molecules from force-displacement curves.

For the important class of intrinsically unstructured proteins [12], entropic forces, such as those considered in the paper, are likely to play an important role.

In previous work we considered polymers confined by impenetrable obstacles of scale invariant shape, such as a polymer attached to the tip of a conical probe approaching a flat surface [13–15]. The reduction in the number of configurations of the polymer leads to a *repulsive* entropic force, which we showed to depend on the (tip to surface) separation  $h$  and the temperature  $T$  as  $F = \mathcal{A}k_B T/h$ . The ‘universal’ amplitude  $\mathcal{A}$  only encodes basic geometrical properties, and gross features of the polymer. For such ‘repulsive’ surfaces, the amplitude  $\mathcal{A}$  is positive. By considering both repulsive and attractive surfaces (as well as by expanding the types of polymers considered), here we demonstrate that attractive surfaces may indeed lead to polymer-mediated attraction with negative  $\mathcal{A}$ .

The interaction of a polymer with a surface can be changed from *repulsive* to *attractive*, e.g. by changing temperature or solvent quality. The competition between energetic attraction and entropic repulsion typically leads to a temperature dependent absorbed layer size, introducing another length into the problem. This length scale diverges at a continuous adsorption transition point introducing a scale-free boundary condition which is distinct from the repulsive surfaces studied previously.

In this paper we expand our formalism [13–16] from the treatment of purely repulsive surfaces to adsorbing surfaces, and to mixed repulsive/adsorbing surface combinations. In Section II we begin examining several polymer types near repulsive or adsorbing *flat* surfaces, and show that the size and sign of the force between a polymer and a surface depends both on the polymer type and the surface type. In Section III we demonstrate that under certain circumstances the polymer-mediated forces between

---

\* Email: kantor@post.tau.ac.il

polymer type \ exponent	$\nu$	$\gamma$	$\gamma_1$	$\gamma_a$
ideal polymer at any $d$	1/2	1	1/2	1
SA polymer at $d = 2$	3/4	43/32	61/64	93/64
SA polymer at $d = 3$	0.588	1.157	0.697	1.304
$\theta$ -polymer at $d = 2$	4/7	8/7	4/7	8/7

TABLE I. Exact (simple fractions) and approximate (decimal fractions) values of exponents of ideal, self-avoiding (SA) and  $\theta$  polymers in free space and close to repulsive or critical attractive *flat* surfaces [17]. (The exponents are defined in the text.)

scale-free surfaces have a universal coefficient, independent of minute details of the polymers. The calculation of force induced by ideal polymers, taken up in Section IV, can be reduced to the solution of a diffusion problem with either absorbing or reflecting boundary conditions. A particularly interesting result is that when all embedded surfaces are at the adsorption transition point, the polymer mediated force is identically zero, independent of shape and geometry. In Sections V and VI we consider a number of examples of mixed repulsive/attractive geometries and demonstrate the ability to modify the force amplitude by changing the surface geometries and types. Finally, in the Discussion section we consider possible generalizations of ideal polymer results to other polymer types.

## II. POLYMERS NEAR ATTRACTIVE OR REPULSIVE FLAT SURFACES

Polymers may exist in different phases, with distinct universal characteristics [18]. At high temperatures in a good solvent polymers expand to maximize the number of available configurations. Ignoring all interactions between monomers, except those imposing its connectivity leads to configurations resembling a random walk; such configurations will be denoted as *ideal* polymers. However, it is unrealistic to ignore the exclusion of monomers from occupying the same volume in space, and the resulting configurations (which are more swollen than ideal random walks) are designated as *self-avoiding* polymers. When the quality of a solvent is reduced, the tendency of monomers to aggregate is akin to an effective short-range attraction which eventually collapses the polymer to a globule of finite density. The transition between good and bad solvent regimes occurs at the so-called  $\theta$ -point, with the resulting configurations labeled as  $\theta$ -polymers.

Ideal, self-avoiding and  $\theta$  polymers are the three polymer types considered in this work, all characterized by (albeit distinct) *universal* scale-invariant properties. For example, they are characterized by a fractal dimension  $d_f = 1/\nu$ , such that the typical separation between monomers  $i$  and  $j$  along the chain scales as  $|i - j|^\nu$ ; the

overall polymer size  $R$  (such as the mean radius of gyration, or the end-to-end distance) grows with the number of monomers  $N$  as  $R = aN^\nu$ , where  $a$  is some microscopic length, of the order of monomer size or persistence length. The exponent  $\nu$  depends only on polymer type, but not on any microscopic details. It ranges from 1/2 to 3/4 depending on space dimension  $d$  and the polymer type, as listed in Table I. This universality enables the frequent use of simple lattice models to study real polymers. E.g., ideal and self-avoiding polymers can be represented by random walks and self-avoiding walks on lattices, respectively, while  $\theta$ -polymers may be represented as self-avoiding walks on a lattice with added attractive interaction between monomers on adjacent lattice sites. (The attractive interaction must then be tuned to exactly match the boundary between good and bad solvents.)

The partition function of polymer types described above is in part universal [18]. It depends on the number of monomers as

$$\mathcal{Z} = bz^N N^{\gamma-1}, \quad (1)$$

where  $b$  and  $z$  depend on microscopic properties of the polymer, while the power-law exponent  $\gamma$  depends only on geometry and polymer type. Thus, the leading *extensive* part of the free energy of a single polymer

$$\mathcal{F} = -k_B T \ln \mathcal{Z} = -k_B T N \ln z - k_B T (\gamma - 1) \ln N + \dots \quad (2)$$

is model dependent, while the coefficient of the *sub-leading*  $\ln N$  is universal. Nevertheless, we shall see that this sub-leading term plays the important role in polymer-mediated forces. In self-avoiding and ideal polymers, the potential energy plays a minor role. In lattice models it is completely absent, and  $\mathcal{Z}$  coincides with the total number of configurations  $\mathcal{N}$ , while  $z$  is the lattice coordination number for random walks, or effective coordination number for self-avoiding walks. The free energy is then obtained from the entropy  $\mathcal{S}$  as  $\mathcal{F} = -T\mathcal{S} = -k_B T \ln \mathcal{N}$ .

If one end of a polymer is attached to an infinite impenetrable flat surface in  $d = 3$ , or to an infinite repulsive line in  $d = 2$ , it will be excluded from half of the space. Nevertheless, the metric exponent  $\nu$  remains unmodified, although the prefactor  $a$  in the power law  $R = aN^\nu$  does change. The number of available configurations, and hence the partition function, is reduced to  $\mathcal{Z}_1 = b_1 z^N N^{\gamma_1-1}$ . Note that the factor  $z$  related to the extensive part of the free energy is unchanged, with the reduction in states captured through the exponent  $\gamma_1 < \gamma$  (see Table I). The change in free energy

$$\Delta \mathcal{F}_1 \equiv \mathcal{F}_1 - \mathcal{F} = k_B T (\gamma - \gamma_1) \ln N \quad (3)$$

is positive, i.e. the polymer is repelled by the wall, or, a force towards the wall needs to be applied to bring the polymer from infinity to the wall.

If the repulsive surface described above is covered by an attractive layer, then a polymer attached by one end

to the surface may decrease its energy by frequently visiting the surface. In discrete models we may simply assign an extra (Boltzmann) weight  $q = e^{-V/k_B T}$ , where  $V < 0$  is the potential at the attractive layer, for each point visited at the boundary. The reduction in entropy of the polymer in this *absorbed* state is compensated by a bigger gain in energy. At high temperatures (or for weakened attractive potential) the entropy wins and the polymer depins from the attractive layer. The free energy per monomer in the absorbed state is lower than that of the free polymer due to the gain in absorption energy, and can be cast as  $-k_B T \ln z_a(T)$  with  $z_a(T) > z$ . If one end of the polymer is held at some moderate distance  $h$  from the surface, a typical configuration will consist of an ‘equilibrium bulk’ attached to the surface, and a strongly stretched tail going from the surface to the point where it is held (with a force of order of  $-(k_B T/a) \ln[z_a(T)/z]$ ). For some computations, it is more convenient to consider a slightly different situation where the polymer is anchored to the surface and pulled away by application of a force [19–21]. In this situation, the behavior of the polymer is different if we control the distance  $h$  *versus* the pulling force applied to its end, akin to controlling density *versus* pressure at a first order liquid-gas transition [19].

The transition from adsorbed to desorbed states occurs at a critical (depinning) temperature  $T_a$  [22–30], where  $z_a(T_a) = z$ . Exactly at  $T_a$ , the partition function of any of the polymer types mentioned [17] above again has a simple form  $\mathcal{Z}_a = b_a z^N N^{\gamma_a - 1}$ . Since almost all monomers are away from the boundary (the fraction of contacts with the boundary increases slower than  $N$ ), the dominant factor of  $z$  remains unchanged. The relation between the exponent  $\gamma_a$  and the free-space  $\gamma$  is not obvious, since the presence of the surface decreases the number of available configuration, which tends to decrease  $\gamma$ , but also decreases the energy, which tends to increase  $\gamma$ . By comparing  $\gamma$  with  $\gamma_a$  in the Table I, we see that for self-avoiding polymers  $\gamma_a > \gamma$ , while for ideal and  $\theta$  polymers  $\gamma_a = \gamma$ . This means that

$$\Delta\mathcal{F}_a \equiv \mathcal{F}_a - \mathcal{F} = k_B T (\gamma - \gamma_a) \ln N, \quad (4)$$

is either negative, i.e., the polymer is attracted by the wall, or vanishes, which makes the wall “invisible” to the polymer that is brought into its vicinity. When  $T$  is not at the adsorption transition point we may expect deviations from the above relations and various crossover effects. However, as long as the correlation length  $\xi$  characterizing the transition [24] exceeds the polymer size, we may treat the system as if it is at  $T_a$ . In the remainder of this article we will always assume that the attractive surfaces are at adsorption transition point without explicitly mentioning this condition.

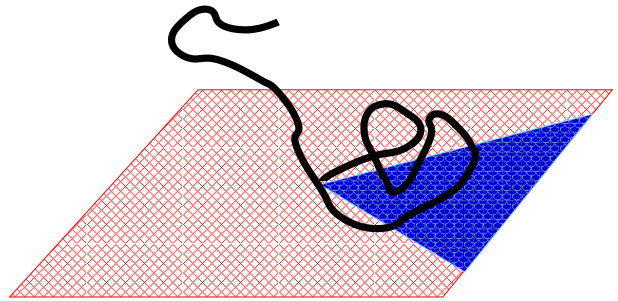


FIG. 1. (Color online) A repulsive surface decorated by a sector with central angle  $2\alpha$  covered by an adsorbing layer. The polymer is attached to the apex of the sector.

### III. POLYMER-MEDIATED FORCES BETWEEN SCALE-FREE SURFACES

The results in the previous section relied on the observation that the partition function of a polymer in free space or near a planar surface (either repulsive or at adsorption transition point) has the form in Eq. (1). This form is a consequence of the fact that the geometries of free space or infinite plane do not possess a characteristic geometrical length scale, i.e., the relevant space is invariant under the coordinate transformation  $\mathbf{r} \rightarrow \lambda \mathbf{r}$ . Similarly, the polymer/surface interactions do not introduce a length scale when they are either repulsive or attractive at adsorption transition point. The same conclusion (hence Eq. (1)) applies to a host of other *scale-free* shapes such as a semi-infinite plane, a sector of a two-dimensional plane in  $d = 3$ , a semi-infinite line, a cone of any cross section, a wedge, or any combinations of such shapes, such as a cone touching a plane. Scale invariance in most such geometries is with respect to a “center” location, such as the apex of a cone or the terminal point of semi-infinite line. We assume that in such cases an attached polymer is anchored to the “center” point to avoid introducing a new length scale. The partition function of a polymer attached to the central point of any scale-free shape will be described by Eq. (1), with an exponent  $\gamma$  that depends on  $d$ , the polymer phase, surface adsorption (repulsive or attractive), and on geometric features characterizing the shape, such as the apex angle  $\Theta$  of the cone [13–15], or the tilt angle of the cone touching a plane [16]. Furthermore, we can mix surface types, by, say, attaching a cone with attractive cover to a repulsive plane. In fact we can have a scale-free situation when a single surface mixes repulsive and attractive regions: E.g., consider a repulsive plane on which a sector has been covered by an attractive layer as in Fig. 1 (with the polymer attached to the sector apex).

Starting from the polymer partition function in scale-free geometries, we can compute polymer-mediated forces between such surfaces. As an example consider a repulsive cone, with a polymer attached to its tip, approaching, say, an attractive plane, as depicted in Fig. 2. When the distance  $h$  between the cone and the plane is signif-

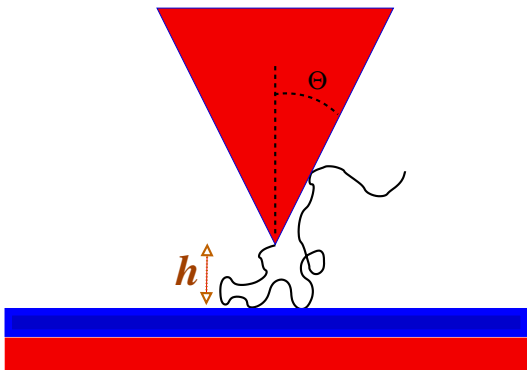


FIG. 2. A polymer (in  $d = 3$ ) attached to the tip of a repulsive solid cone with apex angle  $\Theta$  approaches a plane covered by an attractive (blue) layer. The distance between the plane and the tip of the cone is  $h$ . (This picture can also be interpreted as a two-dimensional wedge approaching a line.)

icantly shorter than the polymer size  $R$ , but larger than the microscopic scale  $a$ ,  $h$  is the only relevant length scale, while  $k_B T$  is the only relevant energy scale. In such a case, the force  $F$  transmitted by the polymer between the surfaces is constrained to be the only dimensionally correct combination

$$F = \mathcal{A} \frac{k_B T}{h}. \quad (5)$$

The dimensionless prefactor  $\mathcal{A}$  (the “force amplitude”) can be positive or negative corresponding to polymer-mediated repulsion or attraction between the objects. (This also follows from various polymer scaling forms [22, 31, 32].) Note that the form of the force (and independence of  $R$ ) is a consequence of the objects having a single point of closest approach. Most of the polymer-surface interactions appear in the neighborhood of this point, while the remote tail of the polymer is not much influenced by the constriction. Equation (5) fails in truly confining geometries; e.g., if confined between parallel planes a distance  $H$  apart, the polymer has nowhere to escape and the total polymer-mediated force can be viewed as a sum of forces exerted by Pincus-de Gennes blobs [33, 34] whose size depends on  $H$ , while their number is proportional to  $N$  [18], leading to a force proportional to  $N$ .

Equation (5) is valid only for  $h$  ranging between  $a$  and  $R$ . When  $h$  decreases and approaches the microscopic size  $a$ , the force saturates at order  $\mathcal{A}k_B T/a$ , while for  $h$  exceeding  $R$  it rapidly drops to 0. Thus, the work that the external force needs to perform to bring the surfaces from far away to a microscopic distance is

$$W = \int_a^R dh \mathcal{A} \frac{k_B T}{h} = \mathcal{A} k_B T \ln \frac{R}{a} = \mathcal{A} \nu k_B T \ln N. \quad (6)$$

(The slight uncertainty in the integration limits is not important since it only affects an additive constant to a term that diverges as  $\ln N$ .) The same work can also be computed from the change in free energies between the

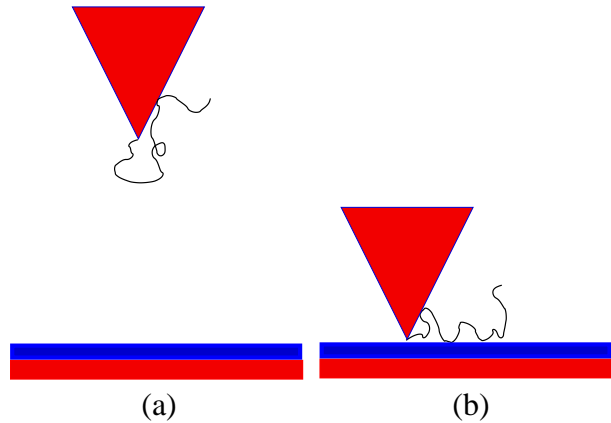


FIG. 3. (Color online) As the cone or wedge depicted in Fig. 2 approaches the surface, it moves between two extreme geometries: (a) When  $h \gg R$  we have a scale-free geometry of a polymer attached to the cone or wedge. (b) Upon touching the surface (or at a microscopic distance  $a$  from it), we arrive at the scale-free geometry of cone/plane.

final and initial states. Both the initial and final states are scale-free as depicted in Fig. 3: Far away only the cone needs to be taken into account, while at the point where the cone touches the plane, we again have a scale-free situation. Therefore, the partition functions in these two extremes will have the form of Eq. (1), but with exponents  $\gamma_{\text{far}}$  and  $\gamma_{\text{near}}$  corresponding to the two limiting geometries, with appropriate polymer and surface types in dimension  $d$ . As in Eqs. (3) and (4) the free energy difference is

$$\Delta \mathcal{F} \equiv \mathcal{F}_{\text{near}} - \mathcal{F}_{\text{far}} = k_B T (\gamma_{\text{far}} - \gamma_{\text{near}}) \ln N. \quad (7)$$

By equating this  $\Delta \mathcal{F}$  with the work  $W$  in Eq. (6) we find

$$\mathcal{A} = \frac{\gamma_{\text{far}} - \gamma_{\text{near}}}{\nu} = \eta_{\text{near}} - \eta_{\text{far}}. \quad (8)$$

In the final step we employed the exponent identity

$$\gamma = (2 - \eta)\nu, \quad (9)$$

to relate the exponent  $\gamma$  to the exponent  $\eta$  characterizing the anomalous decay of density correlations (as  $1/r^{d-2+\eta}$ ). Equation (8) indicates that the force amplitude  $\mathcal{A}$  is a universal quantity akin to critical exponents. In the trivial case, when the polymer, held by a very small probe (point), is moved towards a plane,  $\gamma_{\text{far}}$  coincides with  $\gamma$  of the free space, while  $\gamma_{\text{near}}$  is  $\gamma_1$  or  $\gamma_a$  for repulsive or attractive surfaces, respectively. For example, for a self-avoiding polymer in  $d = 3$  approaching an attracting surface, Eq. (8) with the exponents from Table I leads to  $\mathcal{A} \approx -0.25$ .

The case of purely repulsive boundaries was considered previously for both ideal and self-avoiding polymers. The

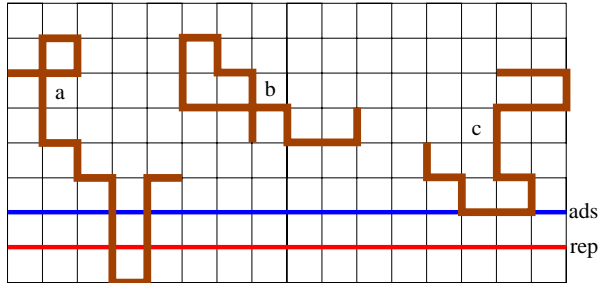


FIG. 4. (Color online) Ideal polymers on a ( $d = 2$ ) square lattice close to a repulsive boundary (red horizontal line denoted “rep”), possibly covered with an adsorbing layer (blue horizontal line denoted “ads”). Configurations that cross or touch the repulsive surface (such as “a”) must be discarded. Those that do not approach either of the surfaces (such as “b”) all have weight 1. In the presence of the attractive (adsorbing) layer, configurations that touch but do not cross this layer gain an extra weight  $q = e^{-V/k_B T}$  for every point on the surface; the configuration “c” thus has weight  $q^3$ .

latter required either numerical simulations or resorting to expansions in  $\epsilon = 4 - d$  [13, 14, 35] to compute the relevant exponents, while ideal polymers could be treated analytically for simple (highly symmetric) geometries [13–15], only requiring simple numerical solutions of diffusion equations for less symmetric scale-free geometries [16].

#### IV. IDEAL POLYMERS NEAR REPULSIVE AND ATTRACTIVE SURFACES

The absence of interactions between non-adjacent monomers of an ideal polymer significantly simplifies its treatment. For an  $N$ -step polymer on a regular lattice with lattice constant  $a$ , such as the square lattice depicted in Fig. 4 with coordination number  $\mu = 4$ , the partition function (beginning at point  $\mathbf{r}$  in free space) is simply the number of configurations  $\mathcal{Z}(\mathbf{r}, \mathcal{N}) = \mathcal{N}(\mathbf{r}, \mathcal{N}) = \mu^N$ . We will define a reduced partition function  $\tilde{\mathcal{Z}} \equiv \mathcal{Z}/\mu^N$ , which in general should scale as  $\tilde{\mathcal{Z}} \sim N^{\gamma-1}$ . In free space  $\tilde{\mathcal{Z}} = 1$ , and therefore  $\gamma = 1$ . The partition function of a polymer of  $(N + 1)$  steps that begins at  $\mathbf{r}$  and ends at  $\mathbf{r}'$  can be calculated recursively as

$$\mathcal{Z}(\mathbf{r}, \mathbf{r}', N + 1) = \sum_{\mathbf{r}'' \text{ nn of } \mathbf{r}'} \mathcal{Z}(\mathbf{r}, \mathbf{r}'', N), \quad (10)$$

with the initial condition  $\mathcal{Z}(\mathbf{r}, \mathbf{r}', 0) = \delta_{\mathbf{r}, \mathbf{r}'}$ . Similarly, the reduced partition function satisfies

$$\begin{aligned} & \tilde{\mathcal{Z}}(\mathbf{r}, \mathbf{r}', N + 1) - \tilde{\mathcal{Z}}(\mathbf{r}, \mathbf{r}', N) \\ &= \frac{1}{\mu} \sum_{\mathbf{r}'' \text{ nn of } \mathbf{r}'} \left[ \tilde{\mathcal{Z}}(\mathbf{r}, \mathbf{r}'', N) - \tilde{\mathcal{Z}}(\mathbf{r}, \mathbf{r}', N) \right]. \quad (11) \end{aligned}$$

For slowly varying functions, we can employ a continuum formulation in which the left hand side is replaced with

a first derivative, while the right hand side represents a second derivative (discrete Laplacian). Regarding the continuous version of  $N$  as a time-like variable  $t$ , the continuum equation for  $\tilde{\mathcal{Z}}$  becomes the diffusion equation for the probability density  $P(\mathbf{r}, \mathbf{r}', t)$  of a diffusing particle that starts its motion at  $\mathbf{r}$  and ends up at  $\mathbf{r}'$  in time  $t$ , which satisfies

$$\frac{\partial P(\mathbf{r}, \mathbf{r}', t)}{\partial t} = D \nabla'^2 P(\mathbf{r}, \mathbf{r}', t), \quad (12)$$

with initial condition  $P(\mathbf{r}, \mathbf{r}', t = 0) = \delta^d(\mathbf{r} - \mathbf{r}')$ . The prime sign on the Laplacian indicates spatial derivatives with respect to  $\mathbf{r}'$ . The diffusion constant  $D$  is chosen such that in free space the mean squared distance coincides with the random walk value of  $\langle (\mathbf{r} - \mathbf{r}')^2 \rangle = a^2 N = 2dDt$  in  $d$  space dimensions, and thus  $D = a^2/2d$ . The probability density  $P$  is related to the discrete probability  $\tilde{\mathcal{Z}}$  by  $\tilde{\mathcal{Z}} = a^d P$ .

In free space all configurations have identical weight. However, in the presence of a *repulsive* wall, such as depicted by the lower (red) horizontal line in Fig. 4, walks that touch or cross that line, such as walk “a” in the figure, must be eliminated from consideration. This can be achieved by applying Eq. (11) only to the points  $\mathbf{r}$  above the repulsive line, while setting  $\tilde{\mathcal{Z}}(\mathbf{r}, \mathbf{r}', N) = 0$ , whenever  $\mathbf{r}'$  is on the repulsive boundary. The continuum limit for  $P$  will then correspond to the solution of Eq. (12) with *absorbing* boundary conditions.

Since the statistical weight of every path is independent of its direction,

$$\tilde{\mathcal{Z}}(\mathbf{r}, \mathbf{r}', N) = \tilde{\mathcal{Z}}(\mathbf{r}', \mathbf{r}, N), \quad (13)$$

i.e. there is symmetry with respect to interchange of the start and end points of the chain. Consequently, in the diffusion equation (12), the prime can be removed from the Laplacian. (This is the usual reciprocity relation of the diffusion problem [36].) After such a change, both sides of the modified Eq. (12) can be integrated over  $\mathbf{r}'$ , the resulting survival probability  $S(\mathbf{r}, t) \equiv \int P(\mathbf{r}, \mathbf{r}', t) d^d \mathbf{r}'$  evolving as

$$\frac{\partial S(\mathbf{r}, t)}{\partial t} = D \nabla^2 S(\mathbf{r}, t), \quad (14)$$

with absorbing boundary conditions. The initial condition for survival probability is  $S(\mathbf{r}, t = 0) = 1$ , everywhere inside the space where the particle can diffuse, and  $S(\mathbf{r}, t) = 0$  on the absorbing boundaries. This quantity coincides with the total reduced partition function  $\tilde{\mathcal{Z}}(\mathbf{r}, N)$ . Our previous works considered a variety of cases with scale-free repulsive boundaries [13–16, 37, 38], while in this work we are mostly interested in attractive boundaries or in mixtures of the two.

When a repulsive surface is covered by an attractive (adsorbing) layer (blue top horizontal line in Fig. 4), every time a polymer visits that layer its statistical weight is increased by a factor  $q = e^{-\beta V}$ , where  $V < 0$  is the energy gain. (For  $q = 1$  the layer has no effect, while

$q < 1$  corresponds to a repulsive potential.) The partition function can now be calculated from

$$\mathcal{Z}(\mathbf{r}, \mathbf{r}', N+1) = x(\mathbf{r}) \sum_{\mathbf{r}'' \text{ nn of } \mathbf{r}'} \mathcal{Z}(\mathbf{r}, \mathbf{r}'', N), \quad (15)$$

where  $x(\mathbf{r}) = q$ , for  $\mathbf{r}$  in the adsorbing layer, and  $x(\mathbf{r}) = 1$ , otherwise. This equation must be supplemented with the initial condition  $\mathcal{Z}(\mathbf{r}, \mathbf{r}', 0) = x(\mathbf{r})\delta_{\mathbf{r}, \mathbf{r}'}$  to ensure reciprocity. The usual diffusion equation, still applicable outside the adsorbing layer, is thus modified by the potential near the layer. It is important to note that the region below the adsorbing layer is still impenetrable, and thus the partition function is strictly zero below the surface.

The phenomenology of polymer adsorption is as follows: For zero temperature ( $q \rightarrow \infty$ ) all monomers are on the adsorbing layer, and the partition function is dominated by the energy contribution. At small, but finite, temperatures parts of the polymer detach from the surface gaining entropy. (We can assume that one end of the polymer is always attached to the surface to avoid discussion of the center of mass entropy.) The average number of visits to the adsorbing layer will be proportional to  $N$  ( $n = cN$ , with  $c$  depending on temperature). Despite the loss of entropy, the energy gain from such visits leads to a partition function  $\mathcal{Z}_a \simeq [z_a(T)]^N \gg \mu^N$  in the *adsorbed* phase. As temperature increases and  $q$  is reduced, there is a point where the decrease in the number of configurations due to the impenetrable boundary is exactly compensated by the extra weight provided by the adsorbing layer to configurations that touch the adsorbing layer. From the perspective of a random walker, the reduction in the number of possible paths by the boundary is exactly made up by the extra weight of the walks that arrive at the attractive potential (blue line) but do not touch the adsorbing boundary (red line).

The adsorption of a *discrete* ideal polymer was studied by Rubín [39, 40]. He determined the transition point  $q_c$ , and demonstrated that for a planar attractive surface  $\mathcal{Z} = \mu^N$ , i.e.  $\gamma_a = 1$ . Comparing the behavior of an ideal polymer at  $T_a$ , to a random walk (diffusion) with *reflecting* boundary conditions, Rubín concluded that for large  $N$  these two problems coincide, although subtle differences remain for small  $N$ . Clearly, in the presence of reflecting boundaries the survival probability of a diffusing particle is always  $S(\mathbf{r}, t) = 1$ , which corresponds to a polymer at the adsorption transition point with  $\tilde{\mathcal{Z}}(\mathbf{r}, N) = 1$ .

The universal aspects of Rubín's results can be captured in the continuum limit, taking advantage of the mapping between configurations of the ideal random walks (path integral), and quantum mechanics of a particle in a potential [41]. In particular the (ideal) polymer adsorption problem is mapped to a quantum particle in a one-dimensional potential of an attractive well adjacent to an impenetrable barrier. Depending on the strength of attraction, such a potential may or may not admit a bound state. The bound state (corresponding to the adsorbed polymer) has a wave-function decaying as

$\psi(z) \sim e^{-\lambda z}$  away from the potential; its energy ( $\propto -\lambda^2$ ) designating the gain in polymer free energy upon adsorption. As the potential is weakened,  $\lambda$  vanishes (linearly in  $T_a - T$ ) indicative of the adsorption transition point. At coarse-grained level, the combination of barrier and potential can be expressed as the mixed (Robin) boundary condition  $\psi' + \lambda\psi = 0$ . Under further coarse-graining, at scales larger than  $\lambda^{-1}$  (irrespective of its sign), this requirement becomes equivalent to the Dirichlet boundary condition  $\psi = 0$ , while for  $\lambda = 0$  (an unstable fixed point under coarse-graining), it is the Neumann boundary condition  $\psi' = 0$ . From the perspective of random walks,  $\psi = 0$  corresponds to absorbing boundaries,  $\psi' = 0$  to reflecting boundaries; both limits are scale-invariant (i.e. such boundaries do not introduce a new length scale to the polymer problem.)

The above considerations lead to the following interesting result: If *all* the confining boundaries and inclusions immersed in a long ideal polymer are at adsorption transition point, and thus in the corresponding diffusion problem all barriers are reflective, then the trivial solution of Eq. (14) is  $S(\mathbf{r}, t) = 1$  for any  $t$ . As this does not depend on the positions of the various obstacles, there can be no polymer-mediated force between them! Note that this is true for arbitrary shapes, and the boundaries do not need to be scale-free. (In the particular case of scale-free surfaces, we note the result  $\gamma_a = 1$  for future reference.)

Analytical solutions of Eqs. (12,14) are available for a number of simple shapes [42]. For scale-free shapes it is convenient to choose a coordinate system centered on the center of symmetry (such as the tip of a cone). The dimensionless survival probability  $S$  can only depend on the dimensionless vector  $\mathbf{w} = \mathbf{r}/\sqrt{Dt}$ . Thus,  $S(\mathbf{r}, t) = H(\mathbf{w})$ , and Eq. (14) reduces to

$$\nabla_{\mathbf{w}}^2 H + \frac{1}{2} \mathbf{w} \cdot \vec{\nabla}_{\mathbf{w}} H = 0, \quad (16)$$

where the subscript  $\mathbf{w}$  indicates derivatives with respect to components of  $\mathbf{w}$ . In terms of these dimensionless variables, either the function  $H$  or its normal derivative vanish on the adsorbing or reflecting surfaces respectively. For some geometries, the solution to Eq. (16) can be expressed in terms of a radial distance  $w$ , and a combination of angular variables, such as the polar angle  $\theta$  and  $(d-2)$  azimuthal angles  $(\phi, \psi, \dots)$ . For  $w \ll 1$ , i.e. for long times  $t$ , the distance dependence is expected to be a simple power law  $w^\eta \Psi(\theta, \phi, \dots)$ . In this limit, the second term in Eq. (16) becomes negligible, and the problem reduces to solving the Laplace equation

$$\nabla_{\mathbf{w}}^2 (w^\eta \Psi) = 0. \quad (17)$$

For small fixed  $\mathbf{r}$  we have  $S \sim t^{-\eta/2}$ , and comparing it with the expected  $\tilde{\mathcal{Z}} \sim N^{\gamma-1}$ , we find that  $\eta = 2(1-\gamma)$ , i.e. it is the same exponent  $\eta$  that appears in Eq. (9) for any polymer type.

Thus obtaining the exponent  $\gamma$ , and the related force amplitude, is reduced to finding  $\eta$  in the solution of

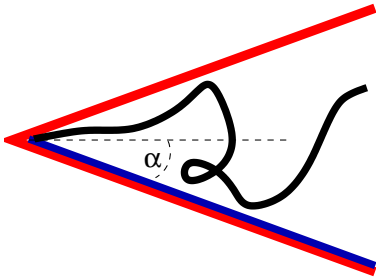


FIG. 5. (Color online) A two-dimensional wedge of inner angle  $2\alpha$ , with a polymer anchored close to its tip. The top side of the wedge is repulsive, while the bottom side is at adsorption transition point.

Eq. (17) with appropriate boundary conditions. If all boundaries are attractive we already know the solution, corresponding to  $\gamma_a = 1$ . If all surfaces are repulsive, the solution to absorbing conditions of the diffusion equation will need to vanish on the boundaries. Problems of this type have been solved for a variety of geometries in the past [13–16, 37, 43]. In the following Sections we consider several examples of mixed boundaries.

## V. TWO-DIMENSIONAL IDEAL POLYMERS NEAR MIXED BOUNDARIES

In a  $d = 2$  scale-free geometry the (Laplace) Eq. (17) simplifies to  $\Psi'' + \eta^2\Psi = 0$ , where prime denotes the derivative of  $\Psi$  with respect to the angle  $\theta$ . This equation is solved by linear combinations of  $\sin(\eta\theta)$  and  $\cos(\eta\theta)$ . For repulsive or attractive boundaries of the polymer problem, we must use boundary conditions of vanishing  $\Psi$  or vanishing derivative  $\Psi'$ , respectively. This should be viewed as an eigenvalue equation, and the primary goal is finding the correct value of  $\eta$ . This equation (complemented by the boundary conditions) has many eigen-solutions. Since  $\Psi$  determines the probability or partition function, its sign cannot change, and consequently we are interested in the “ground state” that corresponds to the lowest value of  $\eta$ .

As an example, consider an ideal polymer anchored close to the central angle  $2\alpha$  of a two dimensional wedge with mixed (repulsive/attractive) boundaries as depicted in Fig. 5. If the angle  $\theta'$  is measured from the lower boundary, then the appropriate solution is  $\Psi = \cos(\pi\theta'/4\alpha)$ , i.e.,

$$\eta = \frac{\pi}{4\alpha} \quad \text{or} \quad \gamma = 1 - \frac{\pi}{8\alpha}, \quad (18)$$

For *two* repulsive boundaries the eigenfunction is  $\Psi = \sin(\pi\theta'/2\alpha)$ , corresponding to

$$\eta = \frac{\pi}{2\alpha} \quad \text{or} \quad \gamma = 1 - \frac{\pi}{4\alpha}. \quad (19)$$

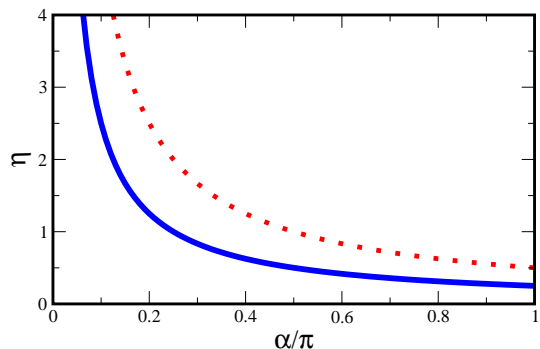


FIG. 6. (Color online) The solid line depicts the exponent  $\eta$  for a mixed repulsive/attractive wedge as depicted in Fig. 5, with opening angle  $2\alpha$ . For comparison, the dotted line depicts  $\eta$  for a wedge with two repulsive boundaries.

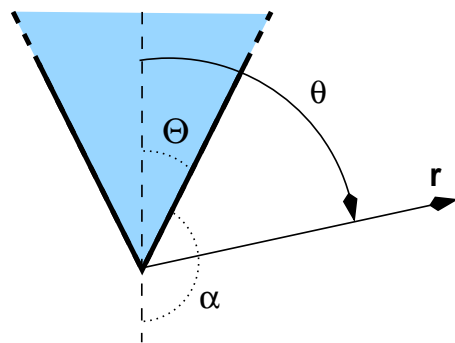


FIG. 7. (Color online) Coordinates for wedge (in  $d = 2$ ) or circular cone (in  $d = 3$ ). The apex angle of a cone/wedge that excludes the polymer is denoted by  $\Theta$ , and its complement by  $\alpha = \pi - \Theta$ . The coordinate angle  $\theta$  will be measured from the axis of the cone/wedge.

Figure 6 depicts the  $\alpha$ -dependence of  $\eta$  both for mixed and for purely repulsive boundaries. Note, that in both cases the exponent diverges in the limit of  $\alpha \rightarrow 0$ , capturing the vanishing of the available states. Equation (18) with  $2\alpha = \pi$ , is the same as Eq. (19) for  $2\alpha = 2\pi$ , both representing a single repulsive semi-infinite line with  $\eta = 1/2$ . This means that in  $d = 2$  the presence of such obstruction does limit the behavior of an ideal polymer. (An obstructed line only has marginal effects in  $d = 3$ .) It is interesting to note that while the mixed wedge is equivalent to a repulsive wedge of twice the angle, it can explore configurations not accessible to the repulsive case with  $2\alpha > 2\pi$ , i.e. beyond what would be possible in  $d = 2$ .

The above results for  $d = 2$  are also applicable to wedges in any dimension  $d$ , since the function  $\Psi$  is independent of coordinates parallel to the edge. In particular, in  $d = 3$  the  $2\alpha = \pi$  case of Eq. (18) corresponds to a plane half of which is repulsive while the other half is attractive, with  $\gamma = 3/4$ .

The above expressions for  $\eta$  enable us to compute the force amplitude  $\mathcal{A}$  in the situation depicted in Fig. 2 in

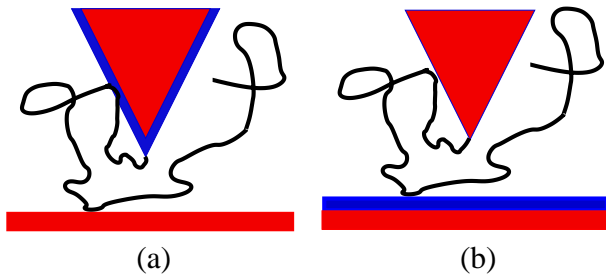


FIG. 8. (Color online) Two variants of cone-plane polymer-mediated setups with mixed boundary conditions: In  $d = 3$  we can have (a) an attractive cone and repulsive plane, or (b) repulsive cone and attractive plane. In  $d = 2$  these drawing can be viewed as a wedge approaching a line.

$d = 2$ , when a wedge with a polymer attached to it approaches an excluded half space. We simply need to find the exponents in the two extreme situations, when the wedge is either far away, or is touching the line. Anticipating the generalization from the wedge in  $d = 2$  to the cone of opening angle  $\Theta$  in  $d = 3$  in the next section, we shall use the notation depicted in Fig. 7. The isolated cone in Fig. 3a has purely repulsive boundaries and is solved by Eq. (19) giving  $\eta_{\text{far}} = \pi/[2(\pi - \Theta)]$ , while the touching of cone and plate in Fig. 3b is described by mixed boundary situation and Eq. (18) results in  $\eta_{\text{near}} = \pi/(\pi - 2\Theta)$ . (We have set  $\alpha \rightarrow \pi - \Theta$  for the repulsive wedge, and  $\alpha \rightarrow \pi/4 - \Theta/2$  in the mixed case.) This results in the force amplitude

$$\mathcal{A} = \frac{\pi^2}{2(\pi - 2\Theta)(\pi - \Theta)}. \quad (20)$$

Note that  $\mathcal{A}$  is always positive, even in the limit of a “needle-like” wedge with  $\Theta \rightarrow 0$ . In the reversed situation where the cone is attractive, while the plane is repulsive,  $\eta = 0$  in the remote configurations but retains the same value as before when the plane and cone are in contact, leading to

$$\mathcal{A} = \frac{\pi}{\pi - 2\Theta}. \quad (21)$$

This amplitude is larger than in the previous example, and in the  $\Theta \rightarrow 0$  limit is the same as a polymer that is brought to the vicinity of a repulsive surface while held at an endpoint *without a wedge*.

## VI. THREE-DIMENSIONAL IDEAL POLYMERS NEAR MIXED BOUNDARIES

In the presence of azimuthal symmetry in three dimensions, as with cones of circular cross section, or such a cone touching a plane and perpendicular to it, the Laplace Eq. (16) simplifies. With  $\Psi$  depending only on the polar angle  $\theta$  as illustrated in Fig. 7, it takes the form

$$(1 - u^2) \frac{d^2 \Psi}{du^2} - 2\mu \frac{d\Psi}{du} + \eta(\eta + 1)\Psi = 0, \quad (22)$$

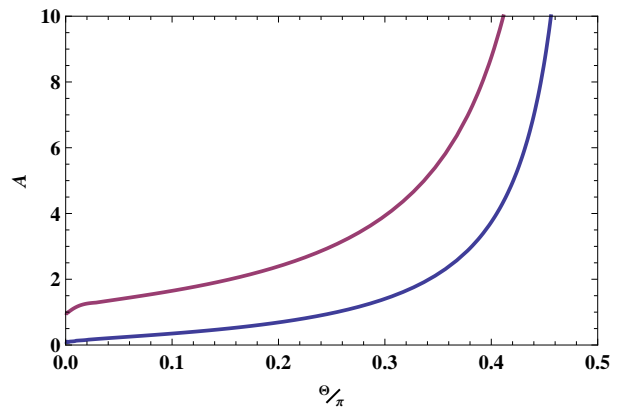


FIG. 9. (Color online) The force amplitude for a three-dimensional cone with apex angle  $\Theta$  approaching a plane. The top curve corresponds to an attractive cone and repulsive plane, while the bottom curve is for a repulsive cone and attractive plane.

where  $u \equiv \cos \theta$ . We seek a regular eigensolution  $\Psi(\theta)$  that vanishes on repulsive boundaries or has a vanishing derivative on attractive boundaries. The general solution to this equation is given by regular (rather than associated) Legendre functions

$$\Psi(\theta) = a_1 P_\eta(u) + a_2 Q_\eta(u). \quad (23)$$

Note that  $P_\eta(1) = 1$  for any  $\eta$ , while  $P_\eta(-1)$  diverges for noninteger  $\eta$ . Similarly,  $Q_\eta(\pm 1)$  is divergent. The linear combination in Eq. (23) can be made regular at -1 by a proper choice of  $a_1/a_2$ . In Refs. [13–15] we described the analytical solutions of this equation for purely repulsive cones, or such cones touching a repulsive plane. (Geometries without azimuthal symmetry can be easily handled numerically [16].)

In many cases, the regularization procedure can be avoided by a convenient choice of functions. For the geometry depicted in Fig. 7, the solution must be regular for  $\Theta \leq \theta \leq \pi$ . Instead of using combinations of  $P_\eta$  and  $Q_\eta$ , we can simply use  $P_\eta(-\cos \theta)$ , which will be regular at  $\cos \theta = -1$ . The value of  $\eta$  for a *repulsive* cone is then determined by requiring

$$P_\eta(-\cos \Theta) = 0. \quad (24)$$

Since  $\Psi$  cannot change sign in the physically permitted region, the smallest possible  $\eta$  must be chosen. This procedure is described in detail in Refs. [13–15]. An attractive boundary requires  $\partial\Psi/\partial\theta$  to vanish at  $\theta = \Theta$ . This, as in all cases of purely attractive boundaries, is trivially achieved by  $\Psi = \text{constant}$ , and  $\eta = 0$ .

Calculation of  $\eta$  for the situation when the cone touches a plane (as in Fig. 3b) is simplified by noting that for non-integer  $\eta$ ,  $P_\eta(u)$  and  $P_\eta(-u)$  are linearly independent and both solve Eq. (22) [44]. Thus for non-integer  $\eta$ , Eq. (23) can be replaced by

$$\Psi(\theta) = P_\eta(\cos \theta) \pm P_\eta(-\cos \theta). \quad (25)$$

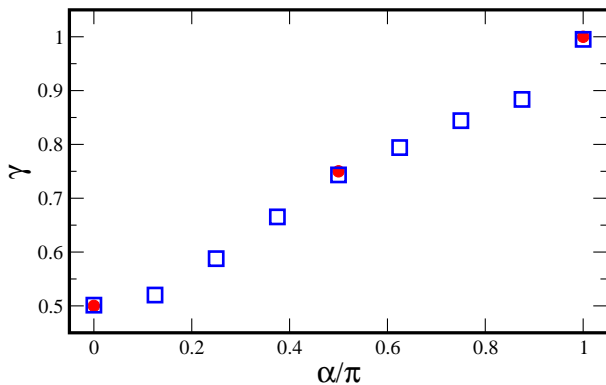


FIG. 10. (Color online) Exponent  $\gamma$  for an ideal polymer attached to a repulsive surface decorated by an attractive sector with the central angle  $2\alpha$ , as depicted in Fig. 1. The adsorbing sector is assumed to be at the adsorption transition point. Open squares depict results of direct numerical estimation of  $\gamma$ , while the full circles represent the exactly known values.

The  $-$  and  $+$  signs enforce vanishing of  $\Psi$  or its derivative at  $\theta = \pi/2$ , respectively, corresponding to a repulsive or attractive plane. The remaining boundary condition at  $\theta = \Theta$  can be implemented by proper choice of the exponent  $\eta(\Theta)$ , which can be obtained numerically. New results pertain to the mixed boundary setups depicted in Fig. 8. (The case of all attractive boundaries is trivial, while that of repulsive boundaries was considered in [13–15].) From knowledge of the values of  $\eta$  in situations depicted in Fig. 8, we can use Eq. (8) to determine the force amplitudes. Figure 9 depicts the force amplitude for the two cases as a function of cone apex angle  $\Theta$ . Similarly, to analogous solution in  $d = 2$  the force amplitude for repulsive plane and attractive cone is larger than that for the reversed situation.

For a less symmetric setup in  $d = 3$ , the Laplace equation Eq. (17) will depend on two angular variables, and implementation of boundary conditions may prove difficult. Fortunately, a direct numerical implementation of Eq. (15), typically only requires a few thousand iterations for a good estimate of  $\gamma$  from the dependence of  $\tilde{Z}$  on  $N$ . As an example we considered a repulsive plane decorated by an attractive sector of opening angle  $2\alpha$  as depicted in Fig. 1, and results from a numerical estimation are shown in Fig. 10. For  $\alpha = 0$  we naturally recover  $\gamma = 1/2$ , as for a purely repulsive plane, while  $\gamma = 1$  for  $\alpha = \pi$ , corresponds to a purely attractive plane. For intermediate angles, the critical exponent simply interpolates between these two limiting values. At  $\alpha = \pi/2$  the plane is divided into repulsive and attractive halves, with  $\gamma = 3/4$  as we found in an equivalent geometry in  $d = 2$ .

## VII. DISCUSSION

In this work we considered several cases of polymer-mediated interactions between repulsive or attractive sur-

faces. While the loss of entropy leads to a repulsive force between impenetrable obstacles, the gain in energy may cause an attractive force for absorbing surfaces. If the confining objects do not introduce a length scale, which is the case for impenetrable obstacles, and surfaces at the adsorption transition point, the entropic force is dimensionally constrained to the form  $\mathcal{A}k_B T/h$  where  $h$  is a characteristic distance between the scale-free surfaces. The amplitude  $\mathcal{A}$  depends on geometry and universality class of the polymer system (ideal, self-avoiding, or  $\theta$  polymer).

A hypothetical setup, such as in Fig. 8, involves a long polymer (or several polymers) of length  $Na$  attached to the tip of a cone at a separation  $h$  from a plane. For an adsorbing surface before the desorption transition, a typical configuration will consist of a nearly straight segment of the polymer stretched from the cone tip to the surface, followed by a much longer segment absorbed to the surface. This situation will hold as long as  $Na \gg h$  and  $Na \gg \xi$ , where  $\xi$  is a characteristic segment size that diverges close to adsorption transition point as  $\xi \propto (T - T_a)^{-1/\phi}$  [22, 24]. The free energy difference between adsorbed and free polymers vanishes at the adsorption transition point as  $\Delta F_a \sim -Nk_B T(a/\xi)$ . The adsorbed polymer also fluctuates away from the surface, forming a layer of thickness  $\ell \propto \xi^\nu$  that also diverges at the adsorption transition point. Equation (5) should apply only in the separation range  $\xi \gg h \gg \ell$ , where the short and long-scale cutoffs are immaterial. On shorter scales, the force should saturate, presumably to order of  $k_B T/\ell$ , while at large scales, the polymer should be stretched, with the force reduced to  $k_B T/\xi$ , corresponding to the loss of free energy per unit length. We thus expect the following sequence of crossovers for the force

$$F = \begin{cases} -\frac{k_B T}{\xi} & \text{if } h \gg \xi \\ \mathcal{A} \frac{k_B T}{\xi} & \text{if } \xi \gg h \gg \ell \\ \sim \pm \frac{k_B T}{\ell} & \text{if } h \ll \ell \end{cases}. \quad (26)$$

(The amplitude  $\mathcal{A}$ , and the sign of the force, is determined by surface and polymer types.) Closer still to the transition, such that  $\xi \sim Na$ , additional crossovers are expected that are not discussed here.

For separations of order of  $0.1\mu\text{m}$  at room temperature, the entropic force is of order  $0.1\text{pN}$ . Forces of such magnitude are now measurable by a host of single molecule manipulation techniques [2–6], e.g. by atomic force microscopes (AFMs) [7], microneedles [8], optical [9, 10] and magnetic [11] tweezers. With a good AFM tip, distances can be measured to accuracy of a few nanometers [6, 45], with forces of order of  $1\text{pN}$  measured in nearly biological conditions [46, 47]. We note that these accuracies fall within the range of entropic forces for fluctuating, featureless polymers described above.

While we considered here the case of a single polymer, related fluctuation-induced forces are also expected in the case of dense melts of long polymers. Such forces have been proposed (dubbed anti-Casimir forces) for dense

polymer melts between parallel plates [48, 49]. For the scale free geometries that we propose, these forces should have the general forms proposed in this paper, albeit with different universal amplitudes.

Finally, we note the interesting observation about the lack of polymer mediated forces for any number of objects (scale-free or not) immersed in *ideal* polymers, as long as all surfaces are at the special adsorption transition point. Compensation of the loss of entropy by marginally attractive energies renders such obstacles invisible to ideal polymers, in a situation similar to index matching of colloids by a fluid of the same dielectric constant. (The van der Waals interaction vanishes in such a case.) It is tempting to imagine that such a situation can also occur for objects in a self-avoiding polymer. However, the

results ( $\gamma_a > \gamma_1$ ) in Table I indicate that  $\mathcal{A} < 0$  for a self-avoiding polymer near a plane at adsorption transition point. Nonetheless, by appropriate coatings of the surfaces (as in Fig. 1) it should be possible to reduce the force prefactor to  $\mathcal{A} = 0$ . Thus there is indeed hope for engineering (at least scale-free) obstacles that are force-free in a self-avoiding polymer solution.

## ACKNOWLEDGMENTS

This work was supported by the National Science Foundation under Grant No. DMR-1206323 (MK), and the Israel Science Foundation grant 453/17 (YK).

- 
- [1] Z. Dogic, *Front. Microbiol.* **7**, 1013 (2016).  
 [2] C. Bustamante, Z. Bryant, and S. B. Smith, *Nature* **421**, 423 (2003).  
 [3] M. S. Kellermayer, *Physiol. Meas.* **26**, R119 (2005).  
 [4] K. C. Neuman, T. Lionnet, and J.-F. Allemand, *Annu. Rev. Mater. Res.* **37**, 33 (2007).  
 [5] A. A. Deniz, S. Mukhopadhyay, and E. A. Lenke, *J. R. Soc. Interface* **5**, 15 (2005).  
 [6] K. C. Neuman and A. Nagy, *Nat. Methods* **5**, 491 (2008).  
 [7] T. E. Fisher, P. E. Marszalek, A. F. Oberhauser, M. Carrion-Vazquez, and J. M. Fernandez, *J. Physiol.* **520**, 5 (1999).  
 [8] A. Kishino and T. Yanagida, *Nature* **334**, 74 (1988).  
 [9] K. Neuman and S. Block, *Rev. Sci. Instrum.* **75**, 2787 (2004).  
 [10] S. Hormeño and J. R. Arias-Gonzalez, *Biol. Cell* **98**, 679 (2006).  
 [11] S. Gosse and V. Croquette, *Biophys. J.* **82**, 3314 (2002).  
 [12] H. J. Dyson and P. E. Wright, *Nat. Rev. Mol. Cell Biol.* **6**, 197 (2005).  
 [13] M. F. Maghrebi, Y. Kantor, and M. Kardar, *Europhys. Lett.* **96**, 66002 (2011).  
 [14] M. F. Maghrebi, Y. Kantor, and M. Kardar, *Phys. Rev. E* **86**, 061801 (2012).  
 [15] Y. Hammer and Y. Kantor, *Phys. Rev. E* **89**, 022601 (2014).  
 [16] N. Alfasi and Y. Kantor, *Phys. Rev. E* **91**, 042126 (2015).  
 [17] E. J. Janse van Rensburg, *The Statistical Mechanics of Interacting Walks, Polygons, Animals and Vesicles*, 2nd ed. (Oxford Univ. Press, 2015).  
 [18] P.-G. de Gennes, *Scaling Concepts in Polymer Physics* (Cornell University Press, Ithaca, New York, 1979).  
 [19] A. M. Skvortsov, L. I. Klushin, A. A. Polotsky, and K. Binder, *Phys. Rev. E* **85**, 031803 (2012).  
 [20] E. J. Janse van Rensburg and S. G. Whittington, *J. Phys. A: Math. Theor.* **46**, 435003 (2013).  
 [21] E. Orlandini and S. G. Whittington, *J. Phys. A: Math. Theor.* **49**, 343001 (2016).  
 [22] E. Eisenriegler, K. Kremer, and K. Binder, *J. Chem. Phys.* **77**, 6296 (1982).  
 [23] K. Binder, in *Phase Transitions and Critical Phenomena*, Vol. 8, edited by C. Domb and J. L. Lebowitz (Academic Press, London, 1983) pp. 1–144.  
 [24] K. De’Bell and T. Lookman, *Rev. Mod. Phys.* **65**, 87 (1993).  
 [25] S. Livne and H. Meirovitch, *J. Chem. Phys.* **88**, 4498 (1988).  
 [26] H. Meirovitch and S. Livne, *J. Chem. Phys.* **88**, 4507 (1988).  
 [27] H. Meirovitch and I. Chang, *Phys. Rev. E* **48**, 1960 (1993).  
 [28] E. Eisenriegler, *Polymers near Surfaces* (World Scientific, Singapore, 1993).  
 [29] T. Vrbová and S. G. Whittington, *J. Phys. A: Math. Theor.* **27**, 3989 (1998).  
 [30] G. Rychlewski and S. G. Whittington, *J. Stat. Phys.* **145**, 6611 (2011).  
 [31] B. Duplantier and H. Saleur, *Phys. Rev. Lett.* **57**, 3179 (1986).  
 [32] P. Rowghanian and A. Y. Grosberg, *J. Phys. Chem. B* **115**, 14127 (2011).  
 [33] P. Pincus, *Macromol.* **9**, 386 (1976).  
 [34] P. G. de Gennes, P. Pincus, R. M. Velasco, and F. Brochard, *J. Phys. (France)* **37**, 1461 (1976).  
 [35] M. Slutsky, R. Zandi, Y. Kantor, and M. Kardar, *Phys. Rev. Lett.* **94**, 198303 (2005).  
 [36] G. H. Weiss, *Aspects and Applications of the Random Walk* (North-Holland, Amsterdam, 1994).  
 [37] Y. Hammer and Y. Kantor, *J. Chem. Phys.* **141**, 204905 (2014).  
 [38] Y. Hammer and Y. Kantor, *Phys. Rev. E* **92**, 062602 (2015).  
 [39] R. J. Rubin, *J. Chem. Phys.* **43**, 2392 (1965).  
 [40] R. J. Rubin, *AIP Conf. Proc.* **109**, 73 (1984).  
 [41] P.-G. de Gennes, *Rep. Prog. Phys.* **32**, 187 (1969).  
 [42] H. S. Carslaw and J. C. Jaeger, *Conduction of Heat in Solids* (Oxford Univ. Press, London, 1959).  
 [43] E. Ben-Naim and P. L. Krapivsky, *J. Phys. A: Math. Theor.* **79**, 495007 (2010).  
 [44] NIST digital library of mathematical functions <http://dlmf.nist.gov/>.  
 [45] H. Kikuchi, N. Yokoyama, and T. Kajiyama, *Chem. Lett.* **26**, 1107 (1997).  
 [46] C. Bustamante, C. Rivetti, and D. Keller, *Curr. Opin. Struct. Biol.* **7**, 709 (1997).  
 [47] B. Drake, C. B. Prater, A. L. Weisenhorn, S. A. Gould,

- T. R. Albrecht, C. F. Quate, D. S. Cannell, H. G. Hansma, and P. K. Hansma, *Science* **243**, 1586 (1989).
- [48] A. N. Semenov and S. P. Obukhov, *J. Phys.: Condens. Matter* **17**, S1747 (2005).
- [49] S. P. Obukhov and A. N. Semenov, *Phys. Rev. Lett.* **95**, 038305 (2005).